HHS Public Access

Author manuscript

Leukemia. Author manuscript; available in PMC 2017 January 06.

Published in final edited form as:

Leukemia. 2017 January ; 31(1): 83–91. doi:10.1038/leu.2016.175.

Combined copy number and mutation analysis identifies oncogenic pathways associated with transformation of follicular lymphoma

Alyssa Bouska[1,*], **Weiwei Zhang**[1,*], **Qiang Gong**[2,*], **Javeed Iqbal**[1], **Anna Scuto**[2], **Julie Vose**[3], **Maja Ludvigsen**[4], **Kai Fu**[1], **Dennis D. Weisenburger**[2], **Timothy C. Greiner**[1], **Randy D. Gascoyne**[5], **Andreas Rosenwald**[6], **German Ott**[7], **Elias Campo**[8], **Lisa M. Rimsza**[9], **Jan Delabie**[10], **Elaine S. Jaffe**[11], **Rita M. Braziel**[12], **Joseph M. Connors**[13], **Chung-I Wu**[14,15], **Louis M. Staudt**[16], **Francesco D'Amore**[17], **Timothy W. McKeithan**[2,#], and **Wing C. Chan**[2,#]

[1]Pathology and Microbiology, University of Nebraska Medical Center, Omaha, NE

[2]Department of Pathology, City of Hope National Medical Center, Duarte, CA

[3]Division of Hematology and Oncology, University of Nebraska Medical Center, Omaha, NE

[4]Department of Biomedicine, Aarhus University, Denmark

[5]Center for Lymphoid Cancer, British Columbia Cancer Agency, Vancouver, BC, Canada

[6]Institute of Pathology, University of Würzburg, and Comprehensive Cancer Center Mainfranken, Würzburg, Germany

[7]Department of Clinical Pathology, Robert-Bosch-Krankenhaus, and Dr. Margarete Fischer-Bosch Institute of Clinical Pharmacology, Stuttgart, Germany

[8]Hematopathology Unit, Hospital Clinic, IDIBAPS, University of Barcelona, Barcelona, Spain

[9]Department of Pathology, University of Arizona, Tucson, AZ

[10]Department of Pathology, University of Toronto, Toronto, Canada

[11]Laboratory of Pathology, Center for Cancer Research, National Cancer Institute, Bethesda, MD

[12]Oregon Health Sciences Center, Portland, OR

[13]Division of Medical Oncology, British Columbia Cancer Agency, Vancouver, BC, Canada

[14]Beijing Institute of Genomics, Chinese Academy of Sciences, Beijing, P.R. China

[15]Department of Ecology and Evolution, University of Chicago, Chicago, IL, 60637, USA

[16]Metabolism Branch, Center for Cancer Research, National Cancer Institute, Bethesda, MD

Correspondence: Wing C. Chan, MD, City of Hope National Medical Center, Department of Pathology, 1500 East Duarte Road, Duarte, CA 91010, jochan@coh.org, Phone: (626) 218-9437, Fax: (626) 301-8842.

*These authors contributed equally to this work.

#These authors contributed equally to this work.

Conflict of interest: The authors declare no conflict of interest.

Supplementary information is available at Leukemia's website

[17]Department of Hematology, Aarhus University Hospital, Denmark

Abstract

Follicular lymphoma (FL) is typically an indolent disease, but 30-40% of FL cases transform into an aggressive lymphoma (tFL) with a poor prognosis. To identify the genetic changes that drive this transformation, we sequenced the exomes of 12 cases with paired FL and tFL biopsies, and identified 45 recurrently mutated genes in the FL-tFL dataset and 39 in the tFL cases. We selected 496 genes of potential importance in transformation and sequenced them in 23 additional tFL cases. Integration of the mutation data with copy-number abnormality (CNA) data provided complementary information. We found recurrent mutations of miR-142, which has not been previously been reported to be mutated in FL/tFL. The genes most frequently mutated in tFL included *KMT2D* (*MLL2*), *CREBBP*, *EZH2*, *BCL2*, and *MEF2B.* Many recurrently mutated genes are involved in epigenetic regulation, the JAK-STAT or the NF-κB pathways, immune surveillance, and cell cycle regulation, or are transcription factors involved in B-cell development. Of particular interest are mutations and CNAs affecting S1P-activated pathways through S1PR1 or S1PR2, which likely regulate lymphoma cell migration and survival outside of follicles. Our custom gene enrichment panel provides high depth of coverage for the study of clonal evolution or divergence.

Keywords

follicular lymphoma; transformed follicular lymphoma; next-generation sequencing; somatic mutation; copy number variations

Introduction

Follicular lymphoma (FL) is the second most common subtype of non-Hodgkin lymphoma (NHL), and about 90% of the cases have the t(14;18) translocation, which results in BCL2 over-expression.[1] In addition to t(14;18), many recurrent chromosomal copy-number abnormalities (CNAs) also occur.[2-7] Although some of the specific genes mutated in FL are known, such as *CREBBP*, *KMT2D* (*MLL2*), and *EZH2*[8-10], others remain to be defined. Next-generation sequencing (NGS) enables us to further clarify which genes and pathways are critical in the development and evolution of FL.

Although FL is usually an indolent disease, around 30-40% of FL cases will transition into an aggressive lymphoma (tFL), most commonly diffuse large B-cell lymphoma (DLBCL)[1], with a poor prognosis. Identification of the genetic changes that drive transformation is key to better understanding the biology of this process and finding pathways to target therapeutically. We previously identified a number of CNAs associated with tFL[7]. To gain a deeper understanding of the spectrum of mutations that occur in FL and tFL, and to define driver mutations associated with critical CNAs, we performed whole exome sequencing (WES) on 12 cases with paired FL and tFL biopsies. From the recurrently mutated genes identified in this study and previously published sequencing studies of other B-cell lymphomas[10-13], we developed a custom gene enrichment panel to sequence specific genes of interest. We sequenced three paired cases whose exomes we had previously sequenced

and 23 additional tFL cases to test the performance of this custom gene panel and determine its usefulness in the study of clonal evolution.

We identified mutations in miR-142 in our series, which have not been reported previously in FL/tFL. We also identified a number of mutations that appear to be more prevalent in tFL. This study provides additional support for the candidate genes and pathways that we and others previously suggested to be important in FL transformation.[7, 14, 15]

Materials and Methods

Patient materials

FL and tFL cases (n=35) with informed consent were identified from the University of Nebraska Medical Center (UNMC), the Lymphoma/Leukemia Molecular Profiling Project (LLMPP), or from Aarhus University Hospital, Aarhus, Denmark. tFL was defined as DLBCL that occurred in a patient previously or concurrently diagnosed with FL. This study was approved by the UNMC Institutional Review Board. Details are summarized in Table S1.

Exome capture and NGS

Exome capture was performed according to the manufacturer's protocol using either Illumina's TruSeq exome enrichment kit (11 paired samples) or Agilent's SureSelect exome enrichment kit (1 paired sample). The equivalent of 1 to 3 exomes was sequenced per lane on an Illumina HiSeq2000 or HiSeq2500 sequencer for an average of 90-fold coverage of coding regions after removing duplicated reads (range: 30×-199×). FASTQ files are available in the NCBI SRA database (SRP074519).

Haloplex custom gene enrichment and NGS

496 genes potentially involved in the FL/tFL disease process were included in the custom panel (Table S2). Criteria for selection included: 1) B-cell expressed genes[16] that were recurrently mutated in the 11 initial WES cases, 2) classic cancer genes (http://cancer.sanger.ac.uk/cancergenome/projects/classic), 3) genes frequently mutated in lymphomas according to the Catalog of Somatic Mutations in Cancer (http://cancer.sanger.ac.uk/cancergenome/projects/cosmic/) or 4) genes recurrently mutated in previously published B-cell lymphoma sequencing studies.[10-13, 17] The custom gene panel was designed using Agilent's SureDesign software (https://earray.chem.agilent.com/suredesign). 200 ng of DNA was used for capture according to the manufacturer's instructions. 10-12 samples were sequenced per lane.

Sequencing data analysis

Raw reads were mapped to the hg19 human genome using the Burrows-Wheeler Aligner (0.7.5a-r405). Genome Analysis Toolkit (v3.1-1-g07a4bf8) was used for local realignment and base quality recalibration. Duplicate marking was done with Picard (v1.115).

Variant calling and filtering were performed with VarScan (v2.3.6). The variants were annotated using ANNOVAR[18]. In order to detect subclonal mutations present at a low

variant-allele frequency (VAF), modifications were made as detailed in the supplement. To obtain a confident somatic variant list, a customized two-step filtering process was applied with integration of CNA data (Supplementary Methods). This pipeline generated a mutation list with two tiers of confidence. Mutations in B-cell-expressed, recurrently mutated genes according to the Tier 1 and 2 lists were rescued to avoid underestimation of prevalence of important genes and designated Tier 3.

Validation of the somatic filters in normal-tumor paired cases

The customized pipeline was validated using a separate dataset with paired normal controls[15]. Somatic mutation lists were generated using (1) our algorithm and two-step filters ignoring the paired normal data and (2) a standard somatic calling pipeline using VarScan 2 (v2.3.6) taking into account the normal data. Comparison between the two lists showed that the false discovery rates of the somatic filters for Tier 1 and 1+2 were 7.3% and 31.6%, respectively, and the false negative rates for Tier 1 and 1+2 were 26.9% and 6.5%.

Gene expression analysis

Gene expression profiling (GEP) data were previously generated at UNMC as part of the Strategic Partnering to Evaluate Cancer Signatures (SPECS)/LLMPP initiatives using HG-U133Plus2.0 arrays according to the manufacturer's protocol (Affymetrix). GEP data is available in NCBI's GEO database (Series GSE81183). See supplementary Methods for additional details.

Results

Genome-wide somatic mutations in exon regions in FL and tFL

685 different genes were mutated in at least one WES sample, but only 449 of these genes appear to be expressed in B-cells according to published data[16] (Table S3). A total of 45 genes (24 expressed) were recurrently mutated in the 12 paired exomes sequenced; 39 genes (21 expressed) were recurrently mutated in the tFL samples (Figure 1; Table 1). We classified mutations found in the tFL biopsy but not in the FL biopsy of a paired case as tFL-only mutations, and identified two genes with recurrent tFL-only mutations, *USH2A* and *TP53* (Figure 1; Table 1).

Deep sequencing using custom gene enrichment

We designed a 496-gene panel (Table S2) and deep sequenced an additional 23 cases, including 15 with only tFL biopsies available. Three paired cases were sequenced with both whole-exome and targeted sequencing platforms, and our results show that all variants found in WES were validated by custom-sequencing (Table S4). The WES results were then integrated with the results from the custom gene enrichment panel (Figure 1; Tables 1, S3 and S5). Analysis of Affymetrix HG-U133Plus2.0 gene expression data in the cases with available data did not reveal any clear correlation of expression level and mutation status for any of the genes; however, the specific expression level of the mutant allele cannot be assessed by microarray data (Figure S1A, Table S3). Given a sample size of n = 35 (WES +custom samples), we can detect mutations occurring at 10% frequency at 97.5% probability.

All paired samples were clearly clonally related as evidenced by high-confidence shared mutations and, in most cases, shared CNAs (Supplementary Figure S2 A-C). In some pairs, however, the FL and tFL have both evolved considerably from their common progenitor, as observed by others.[17, 18]

Though there were some differences in the reported frequency of mutations between our series and others, such as for *TNFRSF14, EZH2,* and *STAT6*[14, 15, 19], the recurrent mutations identified in this series and those in recent FL/tFL sequencing reports[14, 15, 20] were generally highly concordant, affirming the effectiveness of our filtering strategy. We also combined our data with two other published FL/tFL reports[14, 15] to enhance identification of recurrent tFL-only mutations. A gene was classified as a recurrent tFL-only mutation if it was mutated more than once in the combined dataset. We thereby constructed a list of recurrent tFL-only mutations from all available data (Figure 2).

Somatic mutations within regions of recurrent CNAs

Mutations within minimal common regions (MCRs) of recurrent CNAs (Table S6) in FL/tFL[7] were identified. *TNFRSF14* is a likely driver gene in one of the most frequent CNAs in FL and tFL (loss of 1p36.33-p36.31, MCR122). It was mutated in >11% of cases (4 of 35; 8 [23%] including Tier 3 mutations). One mutation in a paired case occurred only in the FL biopsy. The other 3 cases with mutations (excluding Tier 3 cases) were unpaired tFLs. One of the cases had a copy number loss (CNL) affecting *TNFRSF14*. Of the four Tier 3 apparent mutations, two shared mutations were associated with a CNL. Thus, homozygous loss of wild-type *TNFRSF14* is a relatively frequent event in FL and tFL.

Our previous study[7] identified several recurrent losses where the likely driver gene was evident. For example, a MCR of homozygous loss on 6q occurred in 10% of tFLs and included only *TNFAIP3* (Table S6, MCR37)[2, 7]. Three cases were found to have a *TNFAIP3* mutation, indicating that *TNFAIP3* may be inactivated by either CNL or mutation (Figures 1 and S1). A larger heterozygous MCR on 6q occurring in 10% of tFLs includes 102 genes and a recurrent mutation of the kinase *SGK1* (Table S6, MCR340). A small loss on chr16 (in 5% of tFLs) encompasses *CREBBP* and 7 other genes (Table S6, MCR564), and is likely driven by *CREBBP*, the second most frequently mutated gene in our study (19/35 cases; 54%). One case had a shared FL-tFL *CREBBP* mutation and a CNL affecting *CREBBP* in the tFL.

A 17p loss occurs in 9% of FLs and >15% of tFLs (Table S6, MCR593).[7] Seven genes in this region had Tier 1 mutations in our dataset ; however, *TP53* was recurrently mutated only in tFL, involving 26% (9/35) of cases. One case had heterozygous CNL affecting *TP53* in both the FL and tFL (Figure 1, Figure S1B), though the mutation was only in the tFL biopsy. It appears that *TP53* is inactivated by CNL early in the disease process, but mutations likely occur later, as they were only found in tFL.

Somatic mutations acquired during transformation of FL

To identify the genes likely to be involved in transformation, we analyzed the paired cases and identified genes that were only mutated in the tFL biopsies. Among the 12 WES cases, only two recurrently mutated genes were found exclusively in tFL biopsies: *TP53* and

USH2A, but *USH2A* is probably not expressed in B-cells. *TP53* was also affected by CNL as noted above. Expanding the analysis to include all 20 paired cases, we identified two additional genes that were recurrently mutated only in tFL biopsies: *CARD11* and *MLL3*. We also identified a set of genes with tFL-unique mutations in two or more cases, including *EZH2*, *CCND3*, and *MYD88* (Table S5; Figure S3). These mutations were not exclusive to tFL, and some of them are known to occur early in the development of FL. They may represent mutations present as a complement of mutations in the subclone that transformed, or they could occasionally be late mutations that cooperate with other mutations in transformation. Comparing each gene to all the others, three of the 50 genes in Fig. 1 showed a significant difference in the fraction of tFL-mutated paired cases that had a tFL-unique mutation. *TP53* showed a significant increase (p= 0.0022, two-sided Fisher's exact test), consistent with its importance in transformation. In contrast, MLL2 showed a significant decrease (p=0.017) and CREBBP showed a trend toward a decrease (p=0.081), consistent with mutations in these genes usually being early events in FL.

Ten of 20 paired cases had *EZH2* mutations, all of which occurred in the SET domain (Figures 1 & 2). In four of these cases, the mutations were only present in the tFL sample. In five cases, the mutation was shared with the FL biopsy, and in one case the FL biopsy and tFL biopsy each had a distinct mutation (Table S3).

When we combined our data with two published series[14, 15] to gain a more comprehensive view of the genes that likely drive transformation (Figure 2), we identified additional genes that tend to be associated with transformation, including *MYC, EBF1, IRF4, RPN1, SOCS1, SYNE1, SGK1, PIM1, EP300, BMP7, ETS1, SARDH, TAF1, FBX011 and HIST1H1E*.

ABC- and GCB-like tFL and the NF-κB pathway

In our previous study[7], we classified tFLs as activated B-cell (ABC)-like, unclassifiable (UC), or germinal center B-cell (GCB)-like based on gene expression profiling (GEP) using a previously published method[21, 22]. We reported that certain CNAs were more often associated with ABC-like/UC or GCB-like tFL.[7] Classification information was available for 32/35 sequenced cases[7]. The *CD79B* locus was mutated in 14% of cases (5/35) (Figure 3A), more commonly in the ABC-like (40%, 4/10) than in the GCB-like tFL (<5%; 1/21) (p=0.03, Fisher's exact test), consistent with what has been reported for de novo DLBCL.[23]

Because NF-κB pathway activation is a hallmark of ABC-like DLBCL and several mutations that can activate this pathway are preferentially associated with de novo ABC-DLBCL, we investigated these mutations in FL/tFL cases and found mutations in *CARD11* (6/35 cases), *MYD88* (4/35), *TNFAIP3* (3/35), and *BCL10* (1/35). The *CARD11* locus is also commonly affected by gains in FL (24%, n=198) and tFL (39%, n=79), and *TNFAIP3* by losses (26% in FL, 34% in tFL) (Table S8). Most of the *CARD11* mutations we identified occurred within or adjacent to the coiled-coil domain (CCD) (Figure 3B). These mutations likely disrupt binding of the CCD to the inhibitory domain (ID), allowing CARD11 to assume its active conformation even without phosphorylation, and consequently activating NF-κB in the absence of BCR engagement.[24, 25] There was no significant difference in frequency of mutations between ABC-like and GCB-like tFL.

The single *BCL10* mutation (R58Q) occurred in its CARD domain near the acidic patch that binds to the basic patch of the CARD11 CARD domain, and three acidic residues (E50, E53, and E54) were identified as important for binding.[26] The R58Q mutation substitutes a glutamine for the basic arginine, which could increase binding to CARD11 by increasing the net negative charge.

Four of 35 cases (3 with GEP data) had *MYD88* mutations[27]. Two of 10 ABC-like tFLs had a MYD88 mutation compare to 1 of 21 GCB cases. All of the mutations were in the Toll/interleukin-1 homology domain (TIR), including two cases with the most frequent mutation, L265P[27].

BCL2, *MLL2*, *EZH2* and *SOCS1* were mutated more frequently in GCB-like tFL (Table 1). Of note, *BCL2 and SOCS1* were only mutated in GCB-like tFLs, consistent with what has been reported in DLBCL.[12, 28]

Mutations affecting miRNA

Four hundred twenty-two microRNAs were targeted in the exome capture, but only one was found to be mutated in our dataset. *MiR-142* is a hematopoietic-specific microRNA precursor whose 3p and 5p arms are both functional and expressed at similar levels.[29] *MiR-142* was mutated in three of 12 tFL cases, two of which were shared with the corresponding FL. Interestingly, all of the mutations were located in the seed sequences (nucleotides 2-8). One affected miR-142-5p, and two cases had the same mutation affecting miR-142-3p (Figure 3C). The mutation affecting miR-142-3p is identical to one that Kwanhain et al.[30] identified, but the mutation affecting miR-142-5p is novel.

Recurrently targeted pathways

In addition to the NF-κB and p53 pathways described above, our previously identified CNAs strongly implicated B-cell transcription factors (TFs), cell cycle regulation, and immune surveillance in the transformation of FL.[7] Similarly, we found that mutations also commonly target genes involved in these same pathways (Table 2). For example, several regions with small deletions or amplifications were likely driven by B-cell TF)[7] (Table 2). Recurrent mutations affecting B-cell TFs were also identified, including mutation of MEF2B. Four of the cases harbored previously described *MEF2B* mutations[31] that block association with the co-repressor CABIN1, increasing transcriptional activity (3 cases, D83V; 1 case E73K; Figure S3).

We used several bioinformatics programs to identify pathways significantly enriched for mutation in our tFL exome mutation dataset, including David Bioinformatics Resources 6.7. Table S9A shows BIOCARTA and KEGG pathways enriched in our list of mutations. The top three enriched pathways involved B-cell receptor signaling, IL-7 signaling, and JAK-STAT activation. Clustering of gene ontology (GO) categories indicated that genes important for transcriptional regulation were overrepresented (Table S9B). Furthermore, genes involved in chromatin organization and modification were also enriched, as noted recently by others.[14, 15, 20]

In tFL, SWI/SNF members appear to be targets of both mutation and copy loss. *ARID1A* is mutated in 9% of tFL cases (3/35), and our previous study[7] found that 15% of tFL cases have a CNL affecting *ARID1A* (Table S8), including 5% with a small recurrent CNL that encompassed *ARID1A* (and 39 other genes)(Table S6, MCR124). Additionally, 1/35 tFLs had an *ARID1B* mutation and 1/12 cases had *ARID4B* and *ARID5B* mutation (Table S1). A rare, small, recurrent CNL affected *ARID1B* (and one other gene, TableS6, MCR316), but almost 23% of tFLs had a loss on chr6 that included *ARID1B* (Table S8). In addition to SWI/SNF family members, many genes involved in chromatin organization and modification were mutated in our cases (Figure 2), as also observed by others.[14, 15, 20] *EZH2* and *MLL3* mutations were described above.

We also identified frequent CNAs and mutations affecting genes that regulate B-cell migration and AKT/mTOR pathway activation. This pathway has recently been shown to be mutated in DLBCL tumors and cell lines [10-12, 32, 33]. Figure 4 depicts the pathway with S1P interacting with its receptors. One is S1PR2, a G-protein-coupled receptor that signals through the G-protein GNA13, which interacts with a RHO guanine-nucleotide exchange factor, ARHGEF1. Interruption of this pathway promotes migration of B-cells out of the germinal center (GC) and activation of AKT. All three genes were mutated in our dataset (Table S3). The effect of S1P signaling through S1PR1 is the opposite to S1PR2 signaling, and CD69 interacts with and inhibits S1PR1. No mutation in *CD69* or *S1PR1* was detected by us or others, but analysis of our CNA data[7] indicated CNL involving *CD69* in 7.6% of tFLs (Table S8), which could partially reduce the normal inhibitory influence on S1PR1. Indeed, copy loss affecting *S1PR2*, *GNA13*, *ARHGEF1*, *P2RY8*, and/or *CXCR4* loci occurs more frequently in tFL compared to FL [21.5% (n=79) vs 7.5% (n=198), Table S8].

AKT pathway activation can be enhanced by concurrent activating mutations affecting the mTOR pathway. Two cases harbored a shared FL-tFL mutation affecting conserved residues within the switch 1 region of *RRAGC*, and two other studies identified mutations in three FL cases affecting the same region[14, 15](Figure 3D). Additional genes that affect the PI3K/AKT/mTOR pathway were mutated in our dataset including *TSC2, PIK3R1,* and *PTEN*.

Subclonal Mutations

Examination of paired cases revealed a number of genes in which the VAF increased after transformation (Table S7). A graph of the VAFs from a representative case illustrates that the VAF for subclonal mutations fall outside the grouping of VAFs of clonal mutations (Figure S4). Genes that are subclonal in FL but clonal in the tFL biopsy may help drive the transformation process. Several of the genes whose mutations were identified as subclonal in the FL biopsy, such as *CARD11*, *FOXO1*, *HIST1H1E*, and *MYD88,* are recurrently mutated in our dataset and likely important for disease progression. A mutation in *S1PR2*, which as previously mentioned, is involved in germinal center B-cell confinement,[34] was also detected as subclonal in a FL sample but emerged as clonal in the transformed sample, suggesting it may play a role in transformation.

Discussion

Understanding which genetic events drive the transition from FL to tFL is an important step in identifying which patients are at risk for transformation, determining the best course of treatment, and identifying promising targets for new therapies. In this study, we performed WES on 12 cases with paired FL-tFL biopsies and deep target sequencing on 23 additional cases, and identified recurrently mutated genes and pathways that may contribute to the transformation of FL. Only a few mutations appear unique to tFLs. Thus, transformation likely results from a combination of several genetic or epigenetic changes that cooperatively push the FL to become a tFL. Genes more commonly mutated in tFL, and thus likely to participate in transformation, include *TP53*, *EZH2, MYC, CCND3, MLL3,* and *CARD11.* Many of these have also been shown to be mutated in de novo DLBCL. The frequencies of some of these mutations differ however. For example, previous studies found *EZH2* mutation in about 20-25% of GCB-like DLBCLs and FL[35-37], but almost half (16/35) of our tFL cases had a mutation. *EZH2* is a promising candidate gene that promotes transformation when associated with certain additional abnormalities[16].

Our mutation analysis corroborates our previous CNA observations and strongly suggests that activation of the NF-κB pathway is critically important for the transformation of FL. We have demonstrated that tFL may have a GCB- or ABC-like profile and certain genetic abnormalities are associated with each specific subtype.[38] Intriguingly, recent evidence suggests that divergence into more GCB-like or ABC-like patterns may already be present at the FL stage,[39] although it is not clear at what point these cases are in the trajectory to tFL. Certain mutations detected in our study, such as those in *CARD11*, *MYD88*, and *TNFAIP3,* are seen commonly in de novo ABC-DLBCL and are associated with NF-κB activation. They are, therefore, also expected to have similar functional effects in tFL. A correlation with CNA data indicated that some of these key mutations cooperated with CNAs to generate homozygous alterations that amplify their functional consequences, as illustrated by frequent *CARD11* gains and *TNFAIP3* losses.

In addition to the NF-κB pathway, our previously identified CNAs strongly implicated the p53 pathway, B-cell transcription factors, cell cycle regulation, and immune surveillance in the transformation of FL.[7] Similarly, we find that mutations also commonly target genes involved in these same pathways (Supplementary Note).

Loss of GC confinement is a characteristic of tFL, and recent DLBCL sequencing studies have found mutations in several genes that are involved in GC homeostasis according to mouse studies[32-34]. As depicted in Figure 4, mutations and/or CNLs were found affecting *S1PR2*, *GNA13*, *ARHGEF1*, *P2RY8*, *CXCR4*, and *CD69*. Interruption of this pathway promotes migration of B-cells out of the GC and activation of AKT and may be a critical event in the change from a follicular to a diffuse state in the process of transformation. Concomitant activation of the AKT pathway may be important for survival of cells that move out of the GC microenvironment. AKT pathway activation can be enhanced by concurrent activating mutations affecting the mTOR pathway. mTOR complex 1 (mTORC1) senses nutrient levels and integrates multiple signals to activate many cellular processes important for proliferation. We identified mutations in several genes that may activate the

mTOR pathway. RRAGC heterodimerizes with RRAGA or RRAGB and, given adequate amino acid levels, can recruit mTORC1 through RAPTOR to the lysosomal membrane, where mTORC1 can be activated by RHEB[40]. Recurrent RRAGC mutations in FL were very recently reported to activate mTORC1[41]. TSC2 is a GTPase-activating protein (GAP) that inhibits mTORC1 activation by promoting the conversion of RHEB-GTP to RHEB-GDP[42]. Additional genes that were mutated such as *PIK3R1* and *PTEN* also affect the PI3K/AKT/mTOR pathway.

Several genes involved in the JAK-STAT pathway were mutated (Table 2). *SOCS1* and *STAT6* mutations have been reported and their roles discussed [43, 44] (Figure S3), but the role of *STAT3* mutations is more complicated. In ABC-DLBCL, activation of the STAT3 pathway likely serves an oncogenic function,[43, 44] but STAT3 is generally not activated in FL, and BCL6, in fact, represses STAT3 expression. Four mutations were identified in *STAT3,* and Figure S5 shows their location within the STAT3 crystal structure[45]. The K658N substitution within the SH2 domain is identical to an activating mutation previously identified.[43, 46] The case with this mutation was found unclassifiable according to GEP, and this gain-of-function mutation might function as expected for ABC-DLBCL.[43, 47] In contrast, the K340T mutant may interfere with binding to the target sequence[45] and likely represents a loss-of-function mutation. Because the mutant protein retains the ability to dimerize, it likely will have a dominant-negative effect. This mutation was found in a GCB-like tFL where it may act to block further differentiation.

Deregulation and disruption of normal chromatin structure is clearly important in FL[14, 15, 20]. SWI/SNF family members are frequent targets for mutations in a variety of cancers.[48] Our studies show that *ARID1A* and *B* appear to be frequent targets of both mutation and CNL in tFL. Additional genes involved in chromatin organization and modification were also mutated in our cases (Table 2). Among them, *CREBBP* and *MLL2* mutation are common in FL, frequently representing an early event. In contract, *EZH2* mutations are more likely to occur later in the disease and promote transformation, as it was mutated almost twice as frequently in tFL compared to FL. There is evidence of a positive feedback loop between EZH2 and MYC, via a microRNA network, and MYC was found exclusively mutated in tFLs (Figure 2). [49-51] The availability of specific inhibitors for *EZH2* makes it a promising target for treating tFL in the future.

A novel observation in our study was the presence of mutations affecting the seed sequence of *miR-142* in three of 12 tFL cases (Figure 3C). TargetScan 5.2 (http://www.targetscan.org) showed differences in the predicted targets between mutant and WT (Table S10). Both mutations affected nucleotide-8 of the miRNA, and mutation at that position is expected to alter, but not abolish, complementarity to target genes. The mutation shared by two of our cases, affecting miR-142-3p, is identical to one that Kwanhain et al.[30] identified. They found that this mutation results in both loss and gain of function. Novel target sites in the *ZEB2* 3′ UTR modestly down-regulate its expression; however, the mutant also had impaired ability to down-regulate *RAC1* and *ADCY9*. The miR-142-5p mutation we found is novel. It is intriguing that CYLD, a negative regulator of NF-κB, is high on the list of novel predicted targets for the mutated microRNA (Table S10).

In conclusion, we have identified recurrently mutated genes and important pathways that may be affected by mutation and CNAs in tFL. As there are no mutations that are completely unique to tFL, it is clear that a much larger dataset will be needed to decipher what combination of genetic events cooperate to drive an indolent FL to transform into an aggressive tFL. We have provided evidence for the usefulness of a custom gene enrichment panel that would be particularly suitable for a large study and in the evaluation of clonal evolution. Furthermore, investigation of the epigenetic changes associated with mutation of chromatin modifying genes will clarify how they influence the disease process and help identify promising targets for treatment in the future.

Supplementary Material

Refer to Web version on PubMed Central for supplementary material.

Acknowledgments

This work was supported by the Lymphoma Research Foundation Follicular Lymphoma initiative (W.C.C.), Lymphoma SPORE P50CA136411-01-(NCI) (W.C.C); a grant for Global Engagement from the University of Nebraska Foundation (W.C.C.). The University of Nebraska DNA Sequencing Core receives partial support from the NCRR (1S10RR027754-01, 5P20RR016469, RR018788-08) and the National Institute for General Medical Science (NIGMS) (8P20GM103427, GM103471-09). Thanks to Adam Cornish and Robert J. Boissy for initial sequencing analysis assistance.

References

1. Kridel R, Sehn LH, Gascoyne RD. Pathogenesis of follicular lymphoma. J Clin Invest. 2012 Oct 1; 122(10):3424–3431. [PubMed: 23023713]
2. Ross CW, Ouillette PD, Saddler CM, Shedden KA, Malek SN. Comprehensive analysis of copy number and allele status identifies multiple chromosome defects underlying follicular lymphoma pathogenesis. Clin Cancer Res. 2007 Aug 15; 13(16):4777–4785. [PubMed: 17699855]
3. d'Amore F, Chan E, Iqbal J, Geng H, Young K, Xiao L, et al. Clonal evolution in t(14;18)-positive follicular lymphoma, evidence for multiple common pathways, and frequent parallel clonal evolution. Clin Cancer Res. 2008 Nov 15; 14(22):7180–7187. [PubMed: 19010834]
4. Hoglund M, Sehn L, Connors JM, Gascoyne RD, Siebert R, Sall T, et al. Identification of cytogenetic subgroups and karyotypic pathways of clonal evolution in follicular lymphomas. Genes Chromosomes Cancer. 2004 Mar; 39(3):195–204. [PubMed: 14732921]
5. Horsman DE, Connors JM, Pantzar T, Gascoyne RD. Analysis of secondary chromosomal alterations in 165 cases of follicular lymphoma with t(14;18). Genes Chromosomes Cancer. 2001 Apr; 30(4):375–382. [PubMed: 11241790]
6. Cheung KJ, Delaney A, Ben-Neriah S, Schein J, Lee T, Shah SP, et al. High resolution analysis of follicular lymphoma genomes reveals somatic recurrent sites of copy-neutral loss of heterozygosity and copy number alterations that target single genes. Genes Chromosomes Cancer. 2010 Aug; 49(8):669–681. [PubMed: 20544841]
7. Bouska A, McKeithan TW, Deffenbacher KE, Lachel C, Wright GW, Iqbal J, et al. Genome-wide copy number analyses reveal genomic abnormalities involved in transformation of follicular lymphoma. Blood. 2013 Sep 13.
8. Bodor C, Grossmann V, Popov N, Okosun J, O'Riain C, Tan K, et al. EZH2 mutations are frequent and represent an early event in follicular lymphoma. Blood. 2013 Oct 31; 122(18):3165–3168. [PubMed: 24052547]
9. Green MR, Gentles AJ, Nair RV, Irish JM, Kihira S, Liu CL, et al. Hierarchy in somatic mutations arising during genomic evolution and progression of follicular lymphoma. Blood. 2013 Feb 28; 121(9):1604–1611. [PubMed: 23297126]

10. Morin RD, Mendez-Lago M, Mungall AJ, Goya R, Mungall KL, Corbett RD, et al. Frequent mutation of histone-modifying genes in non-Hodgkin lymphoma. Nature. 2011 Aug 18; 476(7360):298–303. [PubMed: 21796119]
11. Lohr JG, Stojanov P, Lawrence MS, Auclair D, Chapuy B, Sougnez C, et al. Discovery and prioritization of somatic mutations in diffuse large B-cell lymphoma (DLBCL) by whole-exome sequencing. Proc Natl Acad Sci U S A. 2012 Mar 6; 109(10):3879–3884. [PubMed: 22343534]
12. Pasqualucci L, Trifonov V, Fabbri G, Ma J, Rossi D, Chiarenza A, et al. Analysis of the coding genome of diffuse large B-cell lymphoma. Nat Genet. 2011 Sep; 43(9):830–837. [PubMed: 21804550]
13. Schmitz R, Young RM, Ceribelli M, Jhavar S, Xiao W, Zhang M, et al. Burkitt lymphoma pathogenesis and therapeutic targets from structural and functional genomics. Nature. 2012 Oct 4; 490(7418):116–120. [PubMed: 22885699]
14. Okosun J, Bodor C, Wang J, Araf S, Yang CY, Pan C, et al. Integrated genomic analysis identifies recurrent mutations and evolution patterns driving the initiation and progression of follicular lymphoma. Nat Genet. 2014 Feb; 46(2):176–181. [PubMed: 24362818]
15. Pasqualucci L, Khiabanian H, Fangazio M, Vasishtha M, Messina M, Holmes AB, et al. Genetics of follicular lymphoma transformation. Cell Rep. 2014 Jan 16; 6(1):130–140. [PubMed: 24388756]
16. Beguelin W, Popovic R, Teater M, Jiang Y, Bunting KL, Rosen M, et al. EZH2 is required for germinal center formation and somatic EZH2 mutations promote lymphoid transformation. Cancer Cell. 2013 May 13; 23(5):677–692. [PubMed: 23680150]
17. Quesada V, Conde L, Villamor N, Ordonez GR, Jares P, Bassaganyas L, et al. Exome sequencing identifies recurrent mutations of the splicing factor SF3B1 gene in chronic lymphocytic leukemia. Nat Genet. 2012 Jan; 44(1):47–52.
18. Wang K, Li M, Hakonarson H. ANNOVAR: functional annotation of genetic variants from high-throughput sequencing data. Nucleic Acids Res. 2010 Sep.38(16):e164. [PubMed: 20601685]
19. Yildiz M, Li H, Bernard D, Amin NA, Ouillette P, Jones S, et al. Activating STAT6 mutations in follicular lymphoma. Blood. 2015 Jan 22; 125(4):668–679. [PubMed: 25428220]
20. Li H, Kaminski MS, Li Y, Yildiz M, Ouillette P, Jones S, et al. Mutations in linker histone genes HIST1H1 B, C, D and E, OCT2 (POU2F2), IRF8 and ARID1A underlying the pathogenesis of follicular lymphoma. Blood. 2014 Jan 16.
21. Lenz G, Wright G, Dave SS, Xiao W, Powell J, Zhao H, et al. Stromal gene signatures in large-B-cell lymphomas. The New England journal of medicine. 2008 Nov 27; 359(22):2313–2323. [PubMed: 19038878]
22. Wright G, Tan B, Rosenwald A, Hurt EH, Wiestner A, Staudt LM. A gene expression-based method to diagnose clinically distinct subgroups of diffuse large B cell lymphoma. Proc Natl Acad Sci U S A. 2003 Aug 19; 100(17):9991–9996. [PubMed: 12900505]
23. Davis RE, Ngo VN, Lenz G, Tolar P, Young RM, Romesser PB, et al. Chronic active B-cell-receptor signalling in diffuse large B-cell lymphoma. Nature. 2010 Jan 7; 463(7277):88–92. [PubMed: 20054396]
24. Lenz G, Davis RE, Ngo VN, Lam L, George TC, Wright GW, et al. Oncogenic CARD11 mutations in human diffuse large B cell lymphoma. Science. 2008 Mar 21; 319(5870):1676–1679. [PubMed: 18323416]
25. Lamason RL, McCully RR, Lew SM, Pomerantz JL. Oncogenic CARD11 mutations induce hyperactive signaling by disrupting autoinhibition by the PKC-responsive inhibitory domain. Biochemistry. 2010 Sep 28; 49(38):8240–8250. [PubMed: 20799731]
26. Li S, Yang X, Shao J, Shen Y. Structural insights into the assembly of CARMA1 and BCL10. PLoS One. 2012; 7(8):e42775. [PubMed: 22880103]
27. Ngo VN, Young RM, Schmitz R, Jhavar S, Xiao W, Lim KH, et al. Oncogenically active MYD88 mutations in human lymphoma. Nature. 2011 Feb 3; 470(7332):115–119. [PubMed: 21179087]
28. Schif B, Lennerz JK, Kohler CW, Bentink S, Kreuz M, Melzner I, et al. SOCS1 mutation subtypes predict divergent outcomes in diffuse large B-Cell lymphoma (DLBCL) patients. Oncotarget. 2013 Jan; 4(1):35–47. [PubMed: 23296022]

29. Landgraf P, Rusu M, Sheridan R, Sewer A, Iovino N, Aravin A, et al. A mammalian microRNA expression atlas based on small RNA library sequencing. Cell. 2007 Jun 29; 129(7):1401–1414. [PubMed: 17604727]
30. Kwanhian W, Lenze D, Alles J, Motsch N, Barth S, Doll C, et al. MicroRNA-142 is mutated in about 20% of diffuse large B-cell lymphoma. Cancer Med. 2012 Oct; 1(2):141–155. [PubMed: 23342264]
31. Ying CY, Dominguez-Sola D, Fabi M, Lorenz IC, Hussein S, Bansal M, et al. MEF2B mutations lead to deregulated expression of the oncogene BCL6 in diffuse large B cell lymphoma. Nat Immunol. 2013 Oct; 14(10):1084–1092. [PubMed: 23974956]
32. Morin RD, Mungall K, Pleasance E, Mungall AJ, Goya R, Huff RD, et al. Mutational and structural analysis of diffuse large B-cell lymphoma using whole-genome sequencing. Blood. 2013 Aug 15; 122(7):1256–1265. [PubMed: 23699601]
33. Muppidi JR, Schmitz R, Green JA, Xiao W, Larsen AB, Braun SE, et al. Loss of signalling via Galpha13 in germinal centre B-cell-derived lymphoma. Nature. 2014 Dec 11; 516(7530):254–258. [PubMed: 25274307]
34. Green JA, Suzuki K, Cho B, Willison LD, Palmer D, Allen CD, et al. The sphingosine 1-phosphate receptor S1P(2) maintains the homeostasis of germinal center B cells and promotes niche confinement. Nat Immunol. 2011 Jul; 12(7):672–680. [PubMed: 21642988]
35. Guo S, Chan JK, Iqbal J, McKeithan T, Fu K, Meng B, et al. EZH2 mutations in follicular lymphoma from different ethnic groups and associated gene expression alterations. Clin Cancer Res. 2014 Jun 15; 20(12):3078–3086. [PubMed: 24634383]
36. Morin RD, Johnson NA, Severson TM, Mungall AJ, An J, Goya R, et al. Somatic mutations altering EZH2 (Tyr641) in follicular and diffuse large B-cell lymphomas of germinal-center origin. Nat Genet. 2010 Feb; 42(2):181–185. [PubMed: 20081860]
37. Ryan RJ, Nitta M, Borger D, Zukerberg LR, Ferry JA, Harris NL, et al. EZH2 codon 641 mutations are common in BCL2-rearranged germinal center B cell lymphomas. PLoS One. 2011; 6(12):e28585. [PubMed: 22194861]
38. Lenz G, Wright GW, Emre NC, Kohlhammer H, Dave SS, Davis RE, et al. Molecular subtypes of diffuse large B-cell lymphoma arise by distinct genetic pathways. Proc Natl Acad Sci U S A. 2008 Sep 9; 105(36):13520–13525. [PubMed: 18765795]
39. Koues OI, Kowalewski RA, Chang LW, Pyfrom SC, Schmidt JA, Luo H, et al. Enhancer sequence variants and transcription-factor deregulation synergize to construct pathogenic regulatory circuits in B-cell lymphoma. Immunity. 2015 Jan 20; 42(1):186–198. [PubMed: 25607463]
40. Zheng X, Liang Y, He Q, Yao R, Bao W, Bao L, et al. Current models of mammalian target of rapamycin complex 1 (mTORC1) activation by growth factors and amino acids. Int J Mol Sci. 2014; 15(11):20753–20769. [PubMed: 25402640]
41. Okosun J, Wolfson RL, Wang J, Araf S, Wilkins L, Castellano BM, et al. Recurrent mTORC1-activating RRAGC mutations in follicular lymphoma. Nat Genet. 2015 Dec 21.
42. Eyre TA, Collins GP, Goldstone AH, Cwynarski K. Time now to TORC the TORC? New developments in mTOR pathway inhibition in lymphoid malignancies. Br J Haematol. 2014 Aug; 166(3):336–351. [PubMed: 24842496]
43. Ding BB, Yu JJ, Yu RY, Mendez LM, Shaknovich R, Zhang Y, et al. Constitutively activated STAT3 promotes cell proliferation and survival in the activated B-cell subtype of diffuse large B-cell lymphomas. Blood. 2008 Feb 1; 111(3):1515–1523. [PubMed: 17951530]
44. Vainchenker W, Constantinescu SN. JAK/STAT signaling in hematological malignancies. Oncogene. 2013 May 23; 32(21):2601–2613. [PubMed: 22869151]
45. Becker S, Groner B, Muller CW. Three-dimensional structure of the Stat3beta homodimer bound to DNA. Nature. 1998 Jul 9; 394(6689):145–151. [PubMed: 9671298]
46. Jerez A, Clemente MJ, Makishima H, Koskela H, Leblanc F, Peng Ng K, et al. STAT3 mutations unify the pathogenesis of chronic lymphoproliferative disorders of NK cells and T-cell large granular lymphocyte leukemia. Blood. 2012 Oct 11; 120(15):3048–3057. [PubMed: 22859607]
47. Huang X, Meng B, Iqbal J, Ding BB, Perry AM, Cao W, et al. Activation of the STAT3 signaling pathway is associated with poor survival in diffuse large B-cell lymphoma treated with R-CHOP. J Clin Oncol. 2013 Dec 20; 31(36):4520–4528. [PubMed: 24220563]

48. Shain AH, Pollack JR. The spectrum of SWI/SNF mutations, ubiquitous in human cancers. PLoS One. 2013; 8(1):e55119. [PubMed: 23355908]

49. Zhao X, Lwin T, Zhang X, Huang A, Wang J, Marquez VE, et al. Disruption of the MYC-miRNA-EZH2 loop to suppress aggressive B-cell lymphoma survival and clonogenicity. Leukemia. 2013 Dec; 27(12):2341–2350. [PubMed: 23538750]

50. Kuser-Abali G, Alptekin A, Cinar B. Overexpression of MYC and EZH2 cooperates to epigenetically silence MST1 expression. Epigenetics. 2014 Apr; 9(4):634–643. [PubMed: 24499724]

51. Zhang X, Zhao X, Fiskus W, Lin J, Lwin T, Rao R, et al. Coordinated silencing of MYC-mediated miR-29 by HDAC3 and EZH2 as a therapeutic target of histone modification in aggressive B-Cell lymphomas. Cancer Cell. 2012 Oct 16; 22(4):506–523. [PubMed: 23079660]

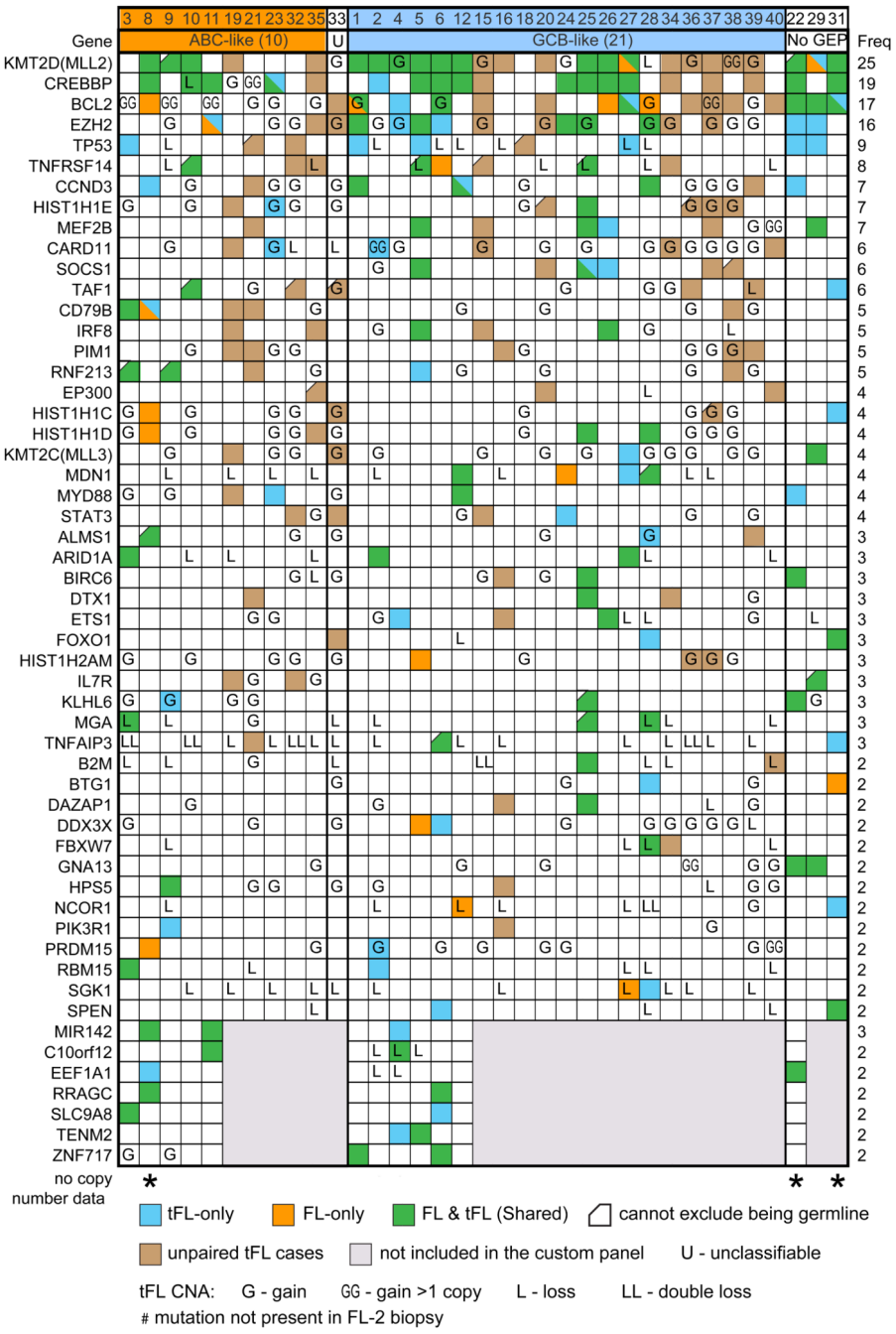

Figure 1.

Genes found to be recurrently mutated specifically in tFLs in 35 FL/tFL cases. Only genes with at least one Tier 1 mutation were included (Materials and Methods). The block color represents the mutation status of the individual cases by gene. Blocks with 2 colors indicate that more than one mutated codon was observed. For example, one case had a truncating mutation and a mutation affecting the initiating methionine codon that occurred on separate alleles, likely resulting in complete loss of functional SOCS1. The other cases had single missense *SOCS1* mutations. Genes also affected by copy number gain or loss in the tFL case

are noted. Copy number data are not available for cases 8, 22, and 31. Tier 3 mutations which were “rescued” from the stringent filtering criteria associated with Tier 1 and 2 mutations are noted as “cannot exclude being germline”.

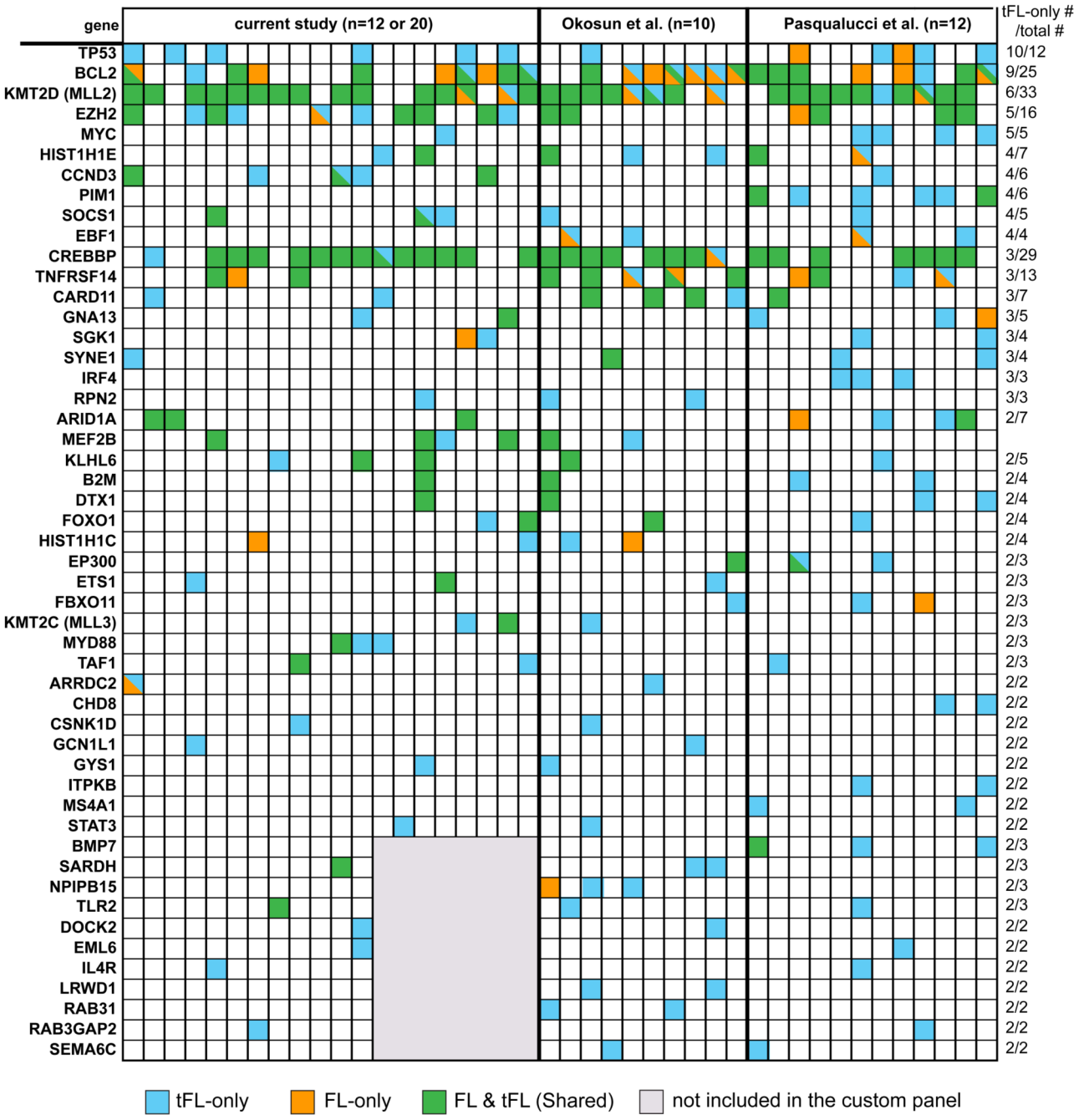

Figure 2.

Diagram of tFL-only mutated genes found in more than two cases. The data were summarized from a combined set of 42 FL/tFL paired cases. Only genes expressed in B-cells[16] are shown. The color of each block represents the mutation type of the corresponding genes and cases.

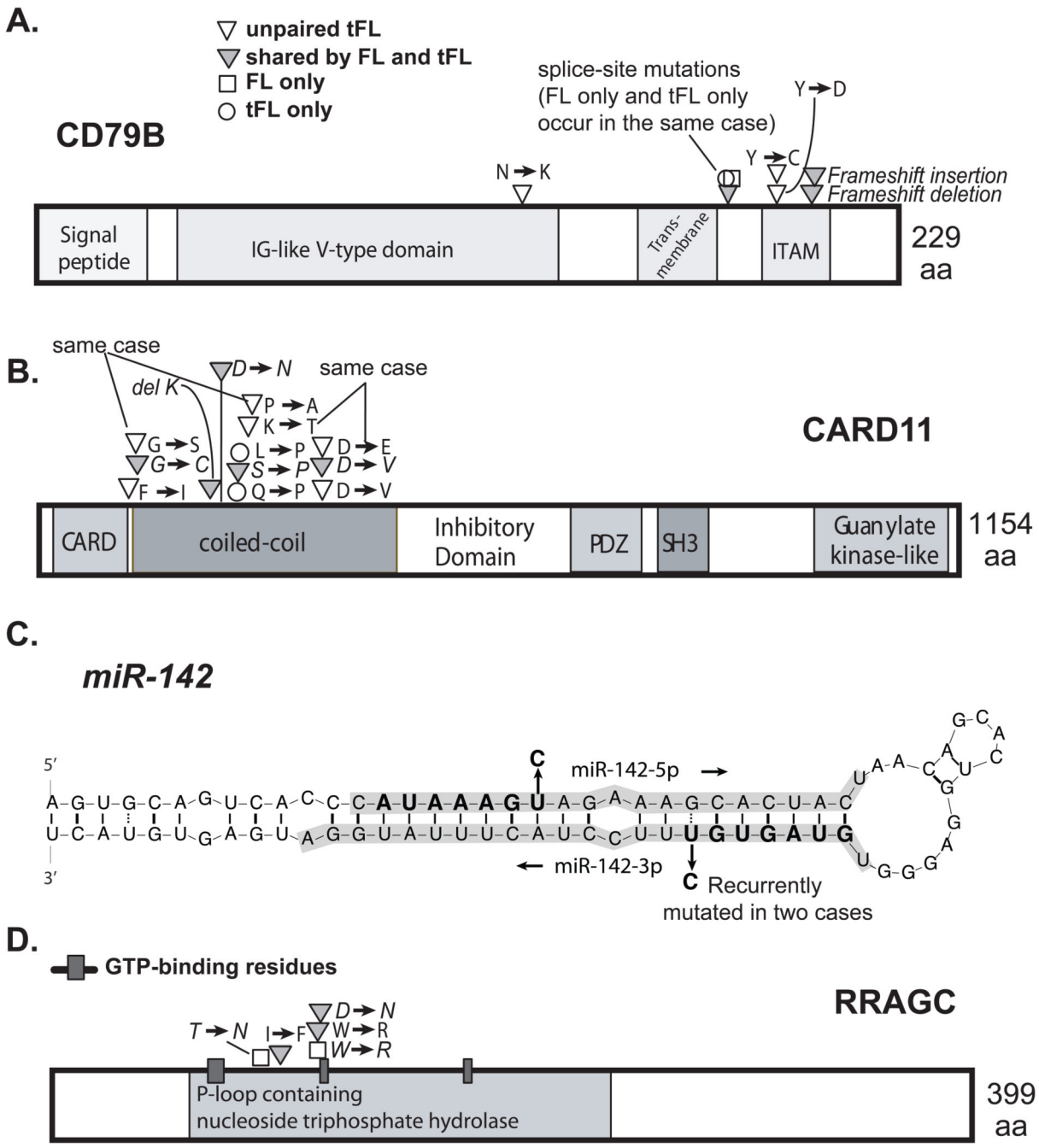

Figure 3.

Schematic of domains/regions affected by mutations for CD79B (A), CARD11 (B), miR-142 (C) and RRAGC (D). The IG-like V-type domain, transmembrane domain, immunoreceptor tyrosine-based activation motif (ITAM), caspase activation and recruitment domain (CARD), coiled-coil domain, inhibitory domain, PDZ domain, SRC homology 3 domain (SH3), guanylate kinase-like domain, and P-loop containing nucleoside triphosphate hydrolase domain are depicted. Sites of GTP binding are noted. The mutations from our case

series are labeled in regular font, while those from the other two published datasets[14, 15] are labeled in italics.

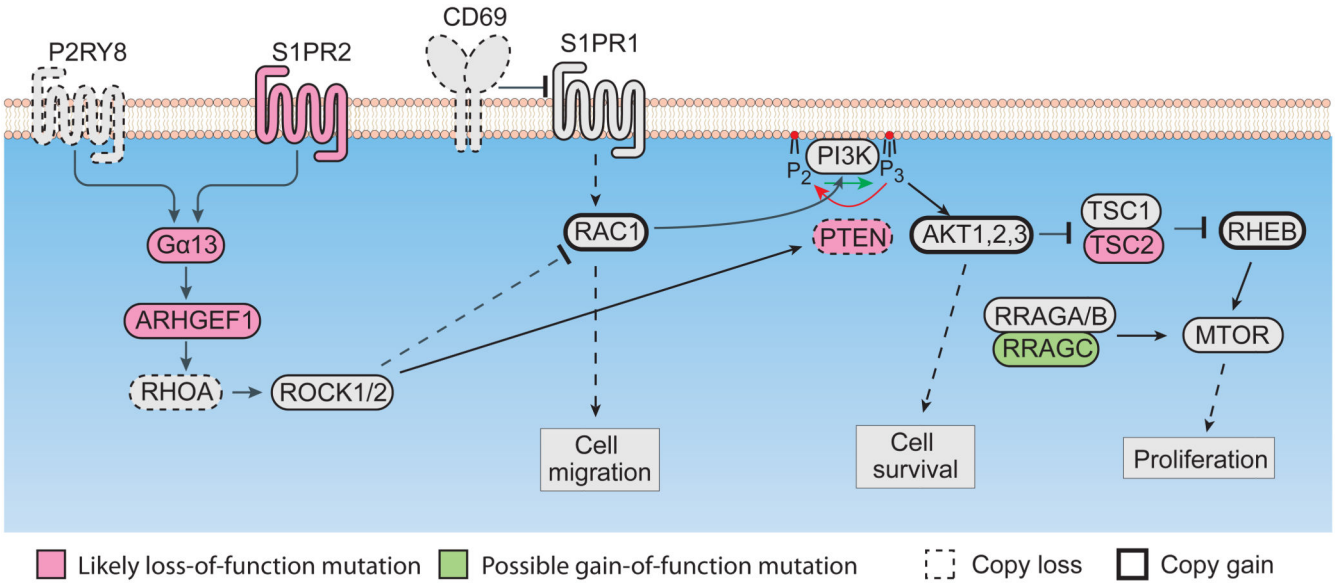

Figure 4.

Abnormalities of the S1PR1 and S1PR2 pathway are associated with FL transformation. Black arrows and bar-headed lines indicate activation or inhibition, respectively; dotted lines indicate an indirect effect. Different color and border lines were used to mark the types of mutations or copy changes observed in our case series (n=35), within which, 80% of the cases carry at least one of the genetic abnormalities. Of note, one case had a mutation in *S1PR2* in the tFL that was subclonal in the FL. That same case had 3 separate FL-tFL shared mutations in *ARHGEF1*. A second case had a shared mutation in *GNA13*. Additionally, Pasqualucci, et al[12] identified GNA13 mutations in 3 cases (2 tFL-unique and 1 FL-unique).

Table 1

Genes mutated in >10% tFLs (expressed in B cells)[1]

Gene	all mut freq (n=*12* or 35)	FL mut freq (n=*12* or 20)	tFL mut freq (n=*12* or 35)	tFL only mut freq (n=*12* or 20)[2]	ABC tFL mut freq (n= *5* or 10)	GCB tFL mut freq (n=*6* or 21)	p-values of ABC vs GCB tFL mutations[3]
KMT2D(MLL2)	71%	75%	71%	0%	50%	81%	0.104544
CREBBP	54%	65%	54%	5%	50%	57%	1
BCL2	49%	45%	40%	5%	10%	57%	0.019974
EZH2	46%	30%	46%	20%	20%	52%	0.1285
TP53	26%	0%	26%	30%	30%	19%	0.651767
TNFRSF14	*23%*	*20%*	*20%*	*0%*	*30%*	*24%*	*1*
CCND3	*20%*	*15%*	*20%*	*10%*	*20%*	*19%*	*1*
HIST1H1E	20%	5%	20%	5%	20%	24%	1
MEF2B	20%	15%	20%	5%	10%	24%	0.634209
CARD11	17%	0%	17%	10%	20%	19%	1
SOCS1	17%	10%	17%	5%	0%	29%	0.141068
TAF1	17%	5%	17%	5%	20%	10%	0.577308
CD79B	14%	10%	14%	0%	40%	5%	0.027438
IRF8	14%	10%	14%	0%	20%	14%	1
PIM1	*14%*	*0%*	*14%*	*0%*	*20%*	*14%*	*1*
RNF213	*14%*	*10%*	*14%*	*5%*	*30%*	*10%*	*0.295514*
EP300	*11%*	*0%*	*11%*	*0%*	*20%*	*10%*	*0.577308*
KMT2C(MLL3)	*11%*	*5%*	*11%*	*5%*	*10%*	*5%*	*1*
MYD88	*11%*	*5%*	*11%*	*10%*	*20%*	*5%*	*0.23693*
STAT3	*11%*	*0%*	*11%*	*5%*	*10%*	*10%*	*1*
HIST1H2AM	*25%*	*8%*	*17%*	*0%*	*0%*	*50%*	*0.181818*
MIR142	*25%*	*17%*	*25%*	*8%*	*40%*	*17%*	*0.545455*
C10orf12	17%	17%	17%	0%	20%	17%	1
EEF1A1	17%	8%	17%	8%	20%	0%	0.454545
HSPG2	17%	8%	17%	8%	0%	33%	0.454545
LEPR	17%	17%	17%	0%	20%	17%	1

Gene	all mut freq (n=*12* or 35)	FL mut freq (n=*12* or 20)	tFL mut freq (n=*12* or 35)	tFL only mut freq (n=*12* or 20)[2]	ABC tFL mut freq (n= *5* or 10)	GCB tFL mut freq (n=*6* or 21)	p-values of ABC vs GCB tFL mutations[3]
RRAGC	17%	17%	17%	0%	20%	17%	1
SLC9A8	17%	8%	17%	8%	20%	17%	1
ZNF208	17%	17%	17%	0%	20%	0%	0.454545
ZNF717	17%	8%	17%	8%	0%	33%	0.454545

[1] The mutation frequencies of genes which are not included in the custom sequencing panel are in italics.

[2] The 15 unpaired tFL cases were not included in the frequency calculation.

[3] The p-values were given by Fisher's exact test based on read counts for any gene mutation preference in ABC versus GCB tFLs.

Table 2
Summary of the altered pathways and processes

Pathways and processes	Representative altered genes
B cell receptor signaling	CARD11, CD19, CD79B, LILRB3, PIK3R1, PPP3R1
IL-7 signal transduction	BCL2, CREBBP, IL2RG, NMI
JAK-STAT pathway	CBL, CCND3, CREBBP, IL2RG, IL4R, PIK3R1, PIM1, PRL, SOCS1, STAT2, STAT3, STAT6
NF-κB pathway	BCL10, CARD11, MYD88, TNFAIP3
TP53 pathway	TP53
Cell cycle regulation	CCND3, PIM1, RB1
Immune surveillance	B2M, CD58, FAS, TNFRSF14
B-cell migration and AKT pathway	ARHGEF1, CD69, GNA13, P2RY8, PTEN, RRAGC, S1PR2, TSC2
Epigenetic regulation	ARID1A, ARID1B, BPTF, BRD8, CABIN1, CHD9, CREBBP, EP300, EP400, EZH2, HDAC5, HUWE1, KDM4D, KDM6A, MLL2 (KMT2D), MLL3 (KMT2C)